Using the Dynamic Energy Budget theory to evaluate the bioremediation potential of the polychaete Hediste diversicolor in an integrated multi-trophic aquaculture system

Helena Lopes Galasso, Sebastien Lefebvre, Catherine Aliaume, Bastien Sadoul, Myriam D. Callier

HAL Id: hal-03410886
https://hal.umontpellier.fr/hal-03410886v1

Submitted on 17 Oct 2022

1 **Using the Dynamic Energy Budget theory to evaluate the bioremediation potential**

2 **of the polychaete *Hediste diversicolor* in an integrated multi-trophic aquaculture**

3 **system**

4 Helena Lopes Galasso[a,b*], Sébastien Lefebvre[c], Catherine Aliaume[d], Bastien Sadoul[a] and

5 Myriam D. Callier[a*]

6

7 [a] MARBEC, Univ Montpellier, CNRS, Ifremer, IRD, Palavas-les-Flots, France

8 [b] CAPES Foundation, Ministry of Education of Brazil, Brasília, DF 70040-020, Brazil

9 [c] Université de Lille, Université Littoral Côte d'Opale, CNRS, Laboratoire

10 d'Océanologie et Géosciences (UMR 8187 LOG), Station Marine de Wimereux, F-

11 59000 Lille, France

12 [d] MARBEC, Univ Montpellier, CNRS, Ifremer, IRD, Montpellier, France

13

14 *Corresponding author at: MARBEC, Univ Montpellier, CNRS, Ifremer, IRD, chemin

15 de Maguelone, F-34250 Palavas-les-Flots, France.

16 E-mail address: myriam.callier@ifremer.fr (M.D. Callier), helenagalasso@gmail.com

17 (H. Galasso)

18

19 **Abstract**

20 Integrated Multi-Trophic Aquaculture (IMTA) systems have been designed to optimize

21 nutrient and energy use, to decrease waste, and to diversify fish-farm production.

22 Recently, the development of detritivorous aquaculture has been encouraged, as

23 detrivores can consume organic particulate matter, reducing benthic eutrophication and

24 the environmental footprint of aquaculture. To this end, the polychaete *Hediste*

25 *diversicolor* is a promising species due to its broad feeding behaviour and its resistance

26 in a wide range of environments. In this study, an existing Dynamic Energy Budget

27 (DEB) model of *H. diversicolor* was used to predict the ragworm's metabolic processes

28 in various environmental conditions and to estimate its bioremediation capacity in an

29 aquaculture context. First, the scaled functional response (*f*) was calibrated in a 98-day

30 growth experiment with two types of food (Fish faeces and Fish feed). Then, we further

31 validated the model using data on the ammonia excretion and oxygen consumption of

32 individuals fed with fish faeces at four different temperatures using the previously

33 calibrated *f*. Overall, we found that the DEB model was able to correctly predict the

34 experimental data (0.51<MRE<0.80). Lastly, different environmental scenarios of

35 seawater temperatures and assimilation rates were compared. The bioremediation

36 potential of *H. diversicolor* was estimated based on cumulated assimilation rates, which

37 could represent 75-289 kg of fish waste year^{-1} for a 100 m^2 ragworm farm (3700 ind. m^{-2}

38). These findings suggest that the DEB model is a promising tool for further IMTA

39 development and management.

40

41 **Keywords:** DEB, deposit feeders, fish waste, metabolism, ragworm, semelparous,

42 bioenergetics

43

1. Introduction

Fed aquaculture can impact ecosystems through the release of organic matter and dissolved nutrients (Hargrave, 2005). One way to minimize aquaculture waste is to develop Integrated Multi-Trophic Aquaculture (IMTA), in which organisms of different trophic levels are co-cultured on the same farm (Chopin et al., 2012). This type of aquaculture can include fed species (e.g. finfish or shrimp) as well as extractive species such as algae that can feed on dissolved inorganic waste generated by the fed species (Abreu et al., 2011; Erler et al., 2000) or filter-feeders and detritivores that can feed on generated organic waste (Jiang et al., 2013; Neori et al., 2004). In open water, particulate organic matter fluxes (faeces and uneaten feed) are mainly vertical (Filgueira et al., 2017) and may accumulate on the bottom sediment both within the farm site and close to it, inducing benthic eutrophication (Hargrave, 2005). The quantity and biochemical composition of the nutrients and organic matter released depends on the cultured species, the farm size, the feed composition, and the rearing conditions (Brigolin et al., 2010).

Using detritivore species in IMTA may improve the mineralization of organic matter through bioturbation processes (Hedman et al., 2011) and feeding (Cammen, 1980), thus preventing benthic eutrophication. The bioremediation potential of several detritivorous species has been evaluated, including fish (Katz et al., 2002; Porter et al., 1996), sea cucumbers (Cubillo et al., 2016; MacDonald et al., 2013; Nelson et al., 2012; Paltzat et al., 2008; Chary et al., 2020), sea urchins (Cook and Kelly, 2007; Orr et al., 2014) and polychaetes (Fang et al., 2017; Marques et al., 2017). Among polychaetes, *Hediste* (*Nereis*) *diversicolor* (O. F. Müller, 1776) has been widely studied (Gillet et al., 2008; Mermillod-Blondin et al., 2004). Similar to other Nereididae, this species plays an important ecological role by constructing burrows in sediment to create galleries.

69 Their bioturbation and ventilation activities promote nutrient fluxes between water and

70 sediment, favouring the oxygenation of the sediment (Michaud et al., 2006) and

71 enhancing organic matter mineralization and nutrient recycling (Heilskov and Holmer,

72 2001). Additionally, *H. diversicolor* can cope with a large range of environmental

73 conditions, in terms of variation in organic matter loading, temperature and salinity

74 (Kristensen, 1983; Ozoh and Jones, 1990). Moreover, its feeding behaviour is

75 diversified: it is considered a detritivore, carnivore, herbivore, suspension feeder and

76 even an optional filter feeder (Nielsen et al., 1995; Riisgård, 1994). More recently, the

77 biomitigation activity of this species has been explored (Cubillo et al., 2016; Marques et

78 al., 2017; Papaspyrou et al., 2010), and studies have demonstrated that individuals can

79 grow significantly when fed on fish waste (Bischoff et al., 2009; Wang et al. 2019).

80 Cubillo et al. (2016) and Marques et al. (2017) have also shown that *H. diversicolor*

81 could assimilate particulate organic matter from fish farms, confirming its potential for

82 IMTA. However, these studies were carried out under specific temperature and salinity

83 conditions, making predicting the bioremediation capacity in other environmental

84 conditions difficult. In this context, mechanistic models can be useful tools as they can

85 simulate physiological and ecological processes under a large range of environmental

86 conditions. Starting from empirical results in a limited number of environmental

87 conditions, this modelling framework allows these results to be extrapolated in order to

88 predict the metabolic responses of individuals in other environmental conditions (Reid

89 et al., 2020). Bioenergetic models are based on the fluxes and conservation of energy in

90 physiological processes, in which energy available for somatic growth is estimated as a

91 result of feeding and excretion (Brett and Groves, 1979). The model chosen in this

92 study was the Dynamic Energy Budget (DEB) model (Kooijman, 2010), which is based

93 on the use of energy by an organism for physiological processes such as food

94 assimilation, growth, maintenance and reproduction. This model has been demonstrated

95 to correctly model the lifecycle of a wide range of species, from bacteria to large

96 mammals. The framework provided by the DEB theory allows the quantification of

97 processes of interest for aquaculture (such as growth and feeding efficiency) and of

98 increasing interest for IMTA (such as the bioremediation capacity of extractive species)

99 (Reid et al., 2020, Chary et al., 2020). The associated DEB parameters for more than

100 2000 modelled species to date are available on the online platform Add-my-Pet (AmP)

101 (www.bio.vu.nl/thb/deb/deblab/add_my_pet). Of these species, 7 are polychaetes, with

102 the recent additions of *Arenicola marina* (De Cubber et al., 2019) and *Hediste*

103 *diversicolor* (Lefebvre, 2019). These DEB model parameters for *H. diversicolor* can

104 now be used to predict metabolic processes under different environmental conditions.

105 The aim of this study was to analyze the mitigation potential of deposit-feeding *H.*

106 *diversicolor* in co-cultivation with finfish. The objectives were (1) to validate the DEB

107 model using new datasets obtained through laboratory experiments on growth rates and

108 ammonia excretion, as well as data on oxygen consumption published independently of

109 the calibration procedure, (2) to evaluate the effects of seawater temperatures (5°C to

110 25°C) and assimilation rates (from *ad libitum* to half an *ad libitum* ration) on some life

111 history traits of *H. diversicolor*, and (3) to quantify the bioremediation potential of *H.*

112 *diversicolor* in different aquaculture contexts.

113

114 **2. Material and methods**

115 **2.1. The DEB theory and the lifecycle of *H. diversicolor***

116 A general presentation of the DEB theory and its mathematical formulation is presented

117 in 'Supplementary material' (see S1). To perform the DEB simulations for *H.*

118   *diversicolor*, we used the available parameters in the AmP database (Lefebvre, 2019)

119   (Table 1), using an abj-model. Essentially, the DEB theory is based on the assumption

120   that assimilated energy first enters a reserve compartment (E). A fixed fraction (κ) of

121   the energy flux coming from the reserve is then utilized, first for somatic maintenance

122   costs and the remaining part for growth of the structural volume (V). The other fraction

123   (1-κ) is spent on maturation (E_H) in juveniles or on reproduction (E_R) in adults, after

124   having paid the maturity maintenance costs (Figure 1). Acquisition processes (i.e.

125   ingestion and assimilation) are linked to the organism's surface area, while somatic

126   maintenance is proportional to its volume. In contrast to the standard version of the

127   DEB model (std), the abj-model considers a metabolic acceleration between birth and

128   metamorphosis (see S1). Consequently, we scaled maximum surface-specific

129   assimilation ($\{\dot{p}_{Am}\}$) and energy conductance ($\dot{v}$) to the organism 's structural length

130   between birth and metamorphosis, following Kooijman et al. (2011). Finally, as it is a

131   semelparous species, *H. diversicolor* dies after its first reproduction (Olive and

132   Garwood, 1981). Therefore, the maximum structural length L_m was the structural length

133   of the animal that attains first reproduction. In DEB theory, authors refer to this

134   reproductive strategy as 'suicide reproduction' (Kooijman, 2010).

135   The DEB model describes changes in the energy content of four state variables (E, V,

136   E_H and E_R for adults), which cannot be measured directly. The volumetric structural

137   length ($L=V^{1/3}$) can be approximated by the shape-corrected physical (observable)

138   length ($\delta_M L_w$). In this study, the length (cm) of the first three segments (L3: the

139   combined length of the prostomium, peristomium and the first setiger) was used as the

140   physical length, as this is more reliable than the total length in polychaetes. Wet weight

141   (WW) was calculated as the sum of the wet mass of the structure and the wet mass of

142   the reserve (see S1). The wet mass of the reproductive buffer was not included in the

143 WW calculation because it was considered negligible most of the time (GSI<3%, see

144 below).

145

2.2. *H. diversicolor* growth performance in controlled environments

147 **2.2.1. Sampling.** *H. diversicolor* individuals were collected in the wild in Arnel

148 Lagoon, on the French Mediterranean coast. The experiments were conducted in the

149 Ifremer marine aquaculture experimental station (Palavas-les-Flots, France). For the

150 oxygen and excretion experiments, individuals were acclimatized for 10 days (see

151 details below). For the growth experiment, *in vitro* reproduction was carried out in

152 October 2016 in order to begin with individuals of the same age. During the early larvae

153 stage (from 0 to 22 days), the polychaete offspring were fed with microalgae (*Chlorella*

154 *sp.*), which were cultured at the experimental station and can be ingested (this was

155 confirmed by microscopic observation of the gut content). Before the beginning of the

156 growth experiment, juveniles (from 22 to 113 days), were fed with fish faeces and

157 raised at temperatures ranging between 15°C and 18°C. This food was chosen because

158 fish farm waste is mainly composed of fish faeces and a varying proportion of uneaten

159 fish feed (Galasso et al., 2017).

160

161 **2.2.2 Growth rates.** The growth experiment was conducted on individuals when they

162 reached 113 days of age; the experiment lasted 98 days (February–April 2017). Two

163 types of feed were tested: faeces from farmed European seabass *Dicentrarchus labrax*

164 (Fish faeces) and commercial fish feed (Fish feed). The collection and preparation of

165 these are detailed in Galasso et al. (2017). The fish faeces were composed of 72%

166 organic matter (OM) (including 3% total organic nitrogen [TON] and 7% total lipids

167 [TL]), and 28% ash. The commercial fish feed was composed of 87% OM (including

168   7% TON and 12% TL) and 12% ash. Polychaetes were fed *ad libitum* (based on the

169   observation of leftover food in the tank) from 48 mg feed.ind^{-1}.d^{-1} to 85 mg.ind^{-1}.d^{-1}

170   (from the beginning to the end of the experiment). The 113 ± 1 day-old individuals

171   (days post-fertilization) at the start of the growth experiment measured on average 1.16

172   ± 0.24 mm L3. Each treatment was performed in small tanks (4 L) in triplicate (6 tanks;

173   18 polychaetes per tank; total of 108 worms). The water temperature was maintained at

174   17 ± 1°C and at a salinity of 18 ± 1 psu (temperature and salinity conditions favourable

175   to *Hediste* growth) (Olivier et al., 1996; Batista et al., 2003). The worms were reared

176   without sediment, but plastic tubes (Ø = 4 mm; several lengths) were added to provide

177   refuge to reduce stress (adapted from Nesto et al., 2018). The tanks were continuously

178   aerated to maintain oxygen concentration close to saturation for the given temperature

179   (Galasso et al., 2018). Individual wet weight was measured on days 177 and 211, and

180   individual L3 length on days 113, 144, 177 and 211. The worms were weighed

181   individually after a fasting period of 24 h to empty their digestive tract. They were then

182   carefully taken from the water using a dip net, cleaned with seawater and dried on paper

183   towels before being weighed on an analytical balance with a precision of 0.001 g.

184   Specific growth rate was calculated as $SGR = \frac{\log WW_f - \log WW_i}{t_f} \times 100$, where WW_i and

185   WW_f is the wet weight (g) at the beginning and the end of the experiment respectively,

186   and *t* is the experiment duration (d) (Hopkins, 1992). A Two-way Anova was performed

187   to test the effect of food type (fixed factor, n= 2, Fish feed and Fish faeces) and tank

188   (random factor, n=3) on WW and L3 at each biometry data. In total, 54 individuals were

189   measured per food type.

190   **2.2.3 Oxygen consumption**. The oxygen consumption rates of the ragworms were

191   recorded as a proxy of the minimal metabolic rate (the standard metabolic rate) at four

192   temperatures (11°C, 17°C, 22°C and 27°C). The oxygen consumption could be

193   considered a proxy of the minimal metabolic rate as it was measured on individuals that

194   had fasted for 24 h in the dark. A detailed description of the experiments and results are

195   presented in Galasso et al. (2018). The individuals ranged from 0.02 to 0.57 g WW, and

196   1.40 to 3.64 mm L3. The polychaetes were acclimatized for 10 days and fed *ad libitum*

197   with seabass *Dicentrarchus labrax* faeces, then acclimatized for 7 days at the

198   experimental temperature conditions. The incubation times were chosen to prevent

199   oxygen saturation from dropping below 80%. Consequently, incubation times varied

200   from 4 h (for the aquariums at 22°C and 27°C) to 5 h (for those at 11°C and 17°C). The

201   results were expressed in µmol/h.

202

203   **2.2.4 Ammonia excretion.** An ammonia excretion experiment was performed

204   simultaneously with oxygen consumption measurements. Water samples (50 mL) were

205   taken at the beginning of the experiment (t_0) (filtered seawater was used to fill the

206   individual chambers) and at the end of incubation (t_f), and immediately frozen at -20°C

207   for further ammonium analyses (N-NH$_4$). The ammonium concentrations were

208   measured using Seal AA3 analytical autoanalyser standard methods (Aminot and

209   Kérouel, 2007) with fluorometric detection (from JASCO, FP-2020plus, France).

210   Ammonia excretion rates were determined following the equation used by Galasso et al.

211   (2018) for oxygen. N-NH$_4$ was transformed to N-NH$_3$ using the conversion factor 1.22

212   (based on molar mass).

213   **2.3. Comparison between predicted and observed data**

214   Simulations were then carried out to compare the output of the model to data from

215   laboratory experiments on growth performance, oxygen consumption ($\dot{j}_O$) and ammonia

216 excretion ($\dot{j}_N$). In DEB theory, $\dot{j}_O$ and $\dot{j}_N$ are weighted sums of three basic fluxes:

217 assimilation ($\dot{p}_A$), dissipation ($\dot{p}_D$) and growth ($\dot{p}_G$) (see S1 for details and equations).

218 First, optimizations of scaled functional response (*f*) were performed to evaluate the

219 assimilation rate of the polychaetes. This was performed using the cma_es function

220 from the cmaes package in R (Trautman et al., 2011) run to minimize the mean relative

221 error (MRE) between predicted and observed data. First an *f* value was obtained for the

222 period prior to the growth experiment (until 113 days of age), and then an *f* value was

223 fitted for each feeding condition (fish faeces or fish feed) in the growth experiment. The

224 last L3 length was not used in the fitting process because of high size-specific mortality

225 related to reproduction. As individuals become green at maturity (Dales, 1950), we used

226 this criteria to remove these individuals from the group and from the dataset. Water

227 temperatures during the different experiments were included in the model.

228 Second, since the oxygen consumption and ammonia excretion experiment was

229 performed using individuals fed on faeces, the *f* fitted using the growth experiment on

230 individuals fed faeces was used for simulating these variables. In addition, as the

231 polychaetes used in the respiration and excretion experiment were collected in the wild,

232 the age and life histories of these individuals were unknown. The scaling with the length

233 and weight was therefore obtained using the DEB model run for individuals with

234 identical life histories (but different ages). Therefore, all the observed differences in

235 lengths within this experiment were linked to differences in age. Finally, since the

236 experiment was performed on polychaetes that had been starved for 24 h, we assumed

237 that the oxygen consumption and ammonia excretion associated to energy assimilation

238 was null ($\dot{p}_A = 0$).

239 **2.4. IMTA scenarios: temperature and assimilation rates**

240 **2.4.1 Effects of temperature and assimilation rate variations**. We evaluated the

241 effects of two key factors that may affect growth: temperature and assimilation rates. As

242 temperature is the main factor in metabolism changes, especially in ectotherms (Wieser,

243 1973), the effect of a large range of temperatures from 5°C to 25°C (in 5°C increments),

244 with fixed optimal feeding conditions (scaled functional response, f=1), was tested. This

245 range was selected based on temperature variations observed in *H. diversicolor* habitats

246 (Scaps, 2002) and temperatures that are recorded in European aquaculture production

247 from Norway to Mediterranean Sea (ex. Brigolin et al. 2014; Wang et al. 2020).

248 Assimilation rates were also tested, with f ranging from 0.5 to 1 (half ration of *ad*

249 *libitum* to full *ad libitum*) (in 0.1 increments), at a constant 20°C temperature.

250 The gonadosomatic index (GSI) is the ratio between gonad mass and total body mass.

251 Using DEB theory, GSI is estimated as the ratio between the reproduction buffer wet

252 mass and the wet weight of the animal (see S1). The GSI could therefore be estimated

253 for each age in the growth experiment. In parallel, survival was recorded during the

254 growth experiment. It was assumed to be mostly related to the spawning event (and the

255 associated death) of the animals. We posited that spawning was triggered above a

256 certain GSI threshold. The survival curve was fitted over time using a sigmoid function

257 with the nls function in R (3.6.2) and Rstudio (1.2.5033). This enabled us to create a

258 link between the estimated GSI and survival. The curve was fitted with a polynomial

259 curve (of degree 5) using the poly function in R in order to obtain links between

260 survival and any GSI. Only the results from the growth experiment using faeces were

261 used for these estimations, since faeces are intended to be the most important food

262 source in a well-designed IMTA system. A GSI of 3% was chosen for the

263 bioremediation simulations since survival was high until this threshold (>90%).

264

265 **2.4.2 Bioremediation capacity.** To estimate the bioremediation capacity of polychaete

266 to consume fish solid wastes**,** total assimilated energy was estimated over a ragworm

267 production cycle (from birth to harvest) in several scenarios (at 20°C with f=0.5 or f=1,

268 and at 5°C and 25°C with f=1). In aquaculture, a good compromise between reaching

269 commercial weight and survival rates has to be found. For each scenario, simulations

270 were either stopped when the GSI reached 3%, or when individual reached 0.5 g WW

271 (minimum polychaete market size, Nesto et al. 2012). Total assimilated energy (J) was

272 then transformed into grams of dry weight (g DW) of faeces considering that the energy

273 content of one g (DW) of fish faeces was 10.4 kJ. We based our estimation on the

274 average composition of seabass faeces: proteins (14%), lipids (4.6%), carbohydrates

275 (12.8%), fibre (40.6%), and ash (28%) (Galasso et al., 2017), and the associated

276 respective energy contents of 23.6 kJ.g^{-1}, 36.2 kJ.g^{-1}, 17.2 kJ.g^{-1}, 8 kJ.g^{-1} and 0 kJ.g^{-1}

277 (Brigolin et al., 2014; Chary et al., 2020). Based on information provided in another

278 study (Scaps, 2002), we considered a population density of 3700 ind.m^{-2} and estimated

279 the bioremediation capacity of a ragworm farm per m^2 for a year-round production,

280 considering the life expectancy of the ragworms and the control of *H. diversicolor*

281 reproduction (Wang et al., 2020).

282 **3. Results and discussion**

283 The results from our simulations obtained for *H. diversicolor* using DEB theory

284 provided a good fit with new empirical data on growth, oxygen consumption and

285 excretion in aquaculture conditions. This new empirical data set was not used for the

286 optimization of the parameters available online (Lefebvre, 2019), and therefore we

287 applied it in order to independently validate the parameter set.

288   **3.1 Growth rates and food quality.** The effect of the two food types, Fish faeces and

289   Fish feed, on the growth rates of *Hediste diversicolor* are presented in Table 2. After 98

290   days of the experiment, polychaetes fed with Fish faeces had a slightly (NS) higher final

291   weight (0.41 ± 0.17 g) and length (L3 = 0.30 ± 0.05 cm) than those fed with Fish feed

292   (WW= 0.36 ± 0.15 g and L3= 0.28 ± 0.06 cm). Significant difference between treatment

293   was only observed on day 177 (two-way Anova test, see Table 2). Individual growth

294   rates (from day 113 to 177) were 0.03 mm L3.d^{-1} and 5 mg WW.d^{-1} (3.8% SGR) for

295   faeces, and 0.02 mm L3.d^{-1} and 4.2 mg WW.d^{-1} (3.5% SGR) for feed. We used the DEB

296   model as an explanatory tool to estimate scaled functional response (*f*) levels in our

297   growth experiment. *f* were estimated at 0.6 and 0.5, for Fish faeces and Fish feed

298   respectively, resulting in slightly higher growth rates for *H. diversicolor* feed with Fish

299   faeces. The DEB simulation fit well with observed length data in the growth experiment

300   (Figure 2), with an MRE of 0.11. In results obtained in other studies, a high variation in

301   growth rates has been observed in relation to food quality. For example, in similar

302   conditions of temperature and salinity (25 psu, 18°C) and for comparable initial weights

303   (50 mg WW), lower growth rates (2.1 mg WW.d^{-1}, 1.8% SGR) were measured for *H.*

304   *diversicolor* fed with macroalgae (Olivier et al., 1996). Meziane and Retiere (2002)

305   obtained even lower growth rates (0.5 to 2.8 mg WW.d^{-1}, 0.3% to 1.9% SGR) for

306   ragworms fed with halophyte detritus in similar environmental conditions (15 psu,

307   21°C). However, Fidalgo e Costa et al. (2000) measured growth rates of 14 mg WW. d^{-1}

308   (5.5% SGR) feeding *H. diversicolor* with a post-larval shrimp diet (15 psu and 20°C).

309   High growth rates (6% to 12% d^{-1} SGR) were also recorded in Nesto et al. (2012), who

310   tested three different sources of food, including Larviva-Biomar® and a seaweed

311   (*Sargassum muticum*, a low-protein food) in *H. diversicolor* cultures. In fact, this last

312   study was used in the parameter estimation procedure for *H. diversicolor* (Lefebvre,

313   2019, Add-my-Pet), considering a maximal functional response for the best food source

314   (f =1). Wang et al. (2019) observed that *H. diversicolor* reared on fish feed (0.025 d^{-1}

315   SGR) grew significantly faster than worms grown on the other diets, including smolt

316   waste (0.012 d^{-1} SGR). The difference between their growth rates and the rates

317   measured in our study may originate from varying food quality and other different

318   experimental conditions, i.e. presence/absence of sediment. Indeed, in our experiment,

319   food was provided *ad libitum*, suggesting that *f*=1. The fitted *f* values of 0.5 and 0.6

320   obtained in our study probably result from a lower digestibility of fish waste compared

321   to other food sources (see Lefebvre et al., 2000). Further experiments could be

322   performed to investigate these hypotheses. Nevertheless, our results showed that despite

323   differences in food quality, growth rates were in the range of other studies. More

324   importantly, although fish waste does not lead to the best SGR compared to other

325   studies, our results indicate that it is a suitable food type for the development, growth

326   and reproduction of *H. diversicolor* in the context of IMTA.

327

328   **3.2 Suicide reproduction and GSI.** It is important to anticipate reproduction,

329   especially when it is associated to death, as is the case for semelparous species. In

330   ragworm aquaculture, harvesting would have to be performed just before reproduction

331   when worms have reached minimum market size (0.5 g WW, Nesto et al., 2012). In our

332   study, observations of the first mortalities attributed to suicide reproduction were made

333   on day 144 (mean survival of 94%). On day 211, mortality reached 43% for individuals

334   fed fish faeces and 52% for individuals fed fish feed. Using DEB simulation, we were

335   able to attribute a GSI to these individuals (Figure 3). We used a GSI of 3% as a

336   threshold for harvesting the individuals during the bioremediation simulations. Indeed,

337   under a GSI of 3%, a survival rate above 90% was estimated (Figure 3). This threshold

338   was estimated from our growth experiment only. Further studies in which GSI is

339   measured on live animals are therefore needed to confirm this threshold. Environmental

340   factors may greatly influence reproduction, including temperature and photoperiod

341   variations (Scaps, 2002; Nesto et al., 2018). In a natural environment, Olive and

342   Garwood (1981) observed the first appearance of developed oocytes in *H. diversicolor*

343   coelom after 18 months. In our study, polychaetes started to reproduce after 5 months,

344   which may indicate that aquaculture conditions with a stable temperature and stable

345   feed input were more favourable to ragworms than natural conditions. Maturation

346   around 4 months under control environment has been observed previously (Nesto et al.,

347   2012). The DEB framework allows simulations to be performed in an environment in

348   which food and temperature vary over time, and therefore estimations of *in situ* age at

349   death (i.e. reproduction) could be performed in the wild as long as temperatures and

350   food conditions are available.

351

352   **3.3 Oxygen consumption and ammonia excretion rates.** The results showed that

353   oxygen consumption (metabolic rate) and ammonia excretion rates increased with body

354   size (WW and L3) and temperature (Figures 4 and 5). The DEB outputs for oxygen

355   consumption and ammonia excretion at different temperatures correctly fit observed

356   data despite the wide variability in oxygen consumption, ranging from 0.09 to 2.35

357   $\mu mol.h^{-1}$ (Figure 4) (Galasso et al., 2018), and ammonia excretion, ranging from 4.10^{-6}

358   to 0.58 $\mu mol.h^{-1}$ (Figure 5). The fit between the oxygen consumption data and the

359   predictions was better than for the ammonia excretion data, with respective MREs of

360   0.51 and 0.80. It appeared that the ammonia results were underestimated by the model.

361   The ammonia results were more scattered than the oxygen consumption rate results. The

362   incubation times was short to keep a good oxygen saturation and concentrations were

363   close to the detection limit. A longer incubation period and no previous starvation may

364   have provided less variable data. In marine species, an increase in ammonia excretion

365   with increased temperature is well known, including for invertebrates (Chen and Lai,

366   1993). In contrast to fish, very little is known regarding the ammonia excretion

367   mechanism and the participating excretory organs in marine invertebrates, especially in

368   polychaetes (Thiel et al., 2017). Thus, our study provides valuable data on this topic,

369   which will need further quantitative data in order to properly characterize nutrient fluxes

370   in IMTAs.

371

372   **3.4 Bioremediation potential.** We found that growth rates increased with increasing

373   temperatures (Figure 6) and scaled functional response (*f*, Figure 7). For the

374   bioremediation estimation, simulations were stopped when GSI reached 3% or 0.5 g

375   WW, considered as the minimum market size. The results from selected scenarios are

376   shown in Table 3. At 20°C, an increased assimilation rate (higher *f*) reduced the time to

377   reach the GSI threshold (99 days with *f*=0.5 vs 79 days with *f*=1). At this stage,

378   ragworms weighed only 0.2 g at *f*=0.5 compared to 0.6 g when *f*=1. At the maximum

379   assimilation rate (*f*=1), increased temperature (5°C vs 25°C) decreased the time to reach

380   a GSI of 3% (163 days at 5°C vs 64 days at 25°C), but had no effect on the final wet

381   weight (0.6 g). Similar observations were made when simulations were stopped at a wet

382   weight of 0.5 g. It should be noted that at 20°C with *f*=0.5, the minimum market size of

383   0.5 g was reached in 128 days, but with a GSI of 3.9%. In a bioremediation perspective,

384   the potential of *H. diversicolor* was estimated based on cumulated assimilation rates

385   ($\dot{p}_A$). Assuming an energy content of 10.4 kJ.g^{-1} DW of seabass faeces, and based on the

386   high density of *H. diversicolor* (3700 ind. m^{-2}) reported in nature (Scaps, 2002), we

387   estimated a bioremediation capacity ranging from 0.23 to 0.87 g faeces DW ind^{-1} year^{-1},

388   eq of 755 to 2887 g faeces DW m^{-2} year^{-1} (Table 3). This could represent 75-289 kg for

389   a 100 m^2 ragworm farm, equivalent to a 2-9 % reduction in the waste produced by a

390   20T seabass farm (160 kg of DW faeces per ton of seabass production, based on

391   assimilation coefficients in Brigolin et al., 2014). This study therefore confirms the

392   potential of *H. diversicolor* in IMTA systems, in particular associated with fish farms,

393   as has been shown in previous studies (Batista et al., 2003; Bischoff et al., 2009; Cubillo

394   et al., 2016 and Marques et al., 2017). Comparisons of bioremediation capacity to other

395   studies are, however, difficult as most of previous studies are site specific or based on

396   specific scenario. The quantity of faeces produced by a marine fish farms depends on

397   numerous factors (species, conversion ratio, temperature, farm management, etc) and

398   can vary from 160 kg of DW faeces per ton of seabass production (Brigolin et al., 2014)

399   to 224 Kg of DW faeces per ton of salmon production (see review by van Rijn, 2013).

400   Wang et al. (2019) estimated that 1 Kg of fish released 250 g of faeces and 30 g of

401   uneaten feed and could produce 800 g of *H. diversicolor*. Considering the feed

402   conversion ratio (g dry faeces used/g polychaete biomass produced) of 3.55 given by

403   the authors, we could estimate a bioremediation capacity of 23 g of fish faeces, eq 9.2 %

404   of faeces reduction (ragworm density was not provided in this study). Chary et al.

405   (2020) compared studies using mathematical models to examine uptake of solid organic

406   matter or nutrients in IMTA systems by other detritivores. Conclusions were quite

407   contrasted (Chary et al., 2020). Cubillo et al. (2016) and Ren et al. (2012) predicted that

408   bottom culture of sea cucumbers could remove more than 70% of the benthic particulate

409   organic carbon (C) from Atlantic salmon (*Salmo salar*) farm units. These two studies

410   did not consider rearing constraints (limit of density) for the extractive species.

411   Including such considerations in models can help predict more realistic production

412   design and bioremediation potentials from extractive species. When considering current

413   density rearing practices, Watanabe et al. (2015) calculated that 4.3% of total particulate

414   nitrogen from milkfish (*Chanos chanos*) culture could be removed by seacumber

415   detritivore species. In the present study, the bioremediation potential was expressed per

416   individual and per m^{-2}, and for a large range of temperature, to allow future

417   comparisons. The DEB model allows simulations to be performed that may be useful to

418   predict life history traits in different environmental conditions, as well as to anticipate

419   harvest before reproduction.

420   **Conclusion.** Our results suggest that fish waste could constitute the exclusive source of

421   food for the polychaete *Hediste diversicolor*. We were able to obtain these results using

422   a DEB model that accurately predicted the species' metabolic processes. Further studies

423   could build on these results by including certain environmental factors, such as water

424   salinity, photoperiod, as well as other water temperature variations that may trigger

425   reproduction. These findings suggest that DEB modelling is a promising tool for IMTA

426   development. The method could help fish producers manage the use of *H. diversicolor*

427   to complement their primary production and could also assist environmental policy by

428   utilizing the bioremediation potential of *H. diversicolor* when associated to fish

429   production.

4. References

Abreu, M.H., Pereira, R., Yarish, C., Buschmann, A.H., Sousa-Pinto, I., 2011. IMTA with *Gracilaria vermiculophylla*: Productivity and nutrient removal performance of the seaweed in a land-based pilot scale system. Aquaculture 312, 77–87. doi:10.1016/j.aquaculture.2010.12.036

Aminot, A., Kérouel, R., 2007. Dosage automatique des nutriments dans les eaux marines.

Batista, F.M., Fidalgo e Costa, P., Ramos, A., Passos, A.M., Pousão Ferreira, P., Cancela da Fonseca, L., 2003. Production of the ragworm *Nereis diversicolor* (O. F. Müller, 1776), fed with a diet for gilthead seabream *Sparus auratus* L., 1758: survival, growth, feed utilization and oogenesis. Inst. Español Oceanogr. 19, 447–451.

Bischoff, A.A., Fink, P., Waller, U., 2009. The fatty acid composition of *Nereis diversicolor* cultured in an integrated recirculated system: Possible implications for aquaculture. Aquaculture 296, 271–276. doi:10.1016/j.aquaculture.2009.09.002

Brett, J.R., Groves, T.D.D., 1979. Physiological Energetics. Vol. VIII- Bioenergetics and Growth, in: Hoar W.S., Randall, D.J., Brett, J.R. (Eds.), Fish Physiology. Academic Press, London, pp. 288–344.

Brigolin, D., Pastres, R., Tomassetti, P., Porrello, S., 2010. Modelling the biomass yield and the impact of seabream mariculture in the Adriatic and Tyrrhenian Seas (Italy). Aquac. Int. 18, 149–163. https://doi.org/10.1007/s10499-008-9232-4

Brigolin, D., Meccia, V. L., Venier, C., Tomassetti, P., Porrello, S.,Pastres, R., 2014. Modelling biogeochemical fluxes across a Mediterranean fish cage farm. Aquaculture Environment Interactions 5(1): 71-88.

Cammen, L.M., 1980. The significance of microbial carbon in the nutrition of the deposit feeding Polychaete *Nereis succinea*. Mar. Biol. 61, 9–20.

Chary, K., Aubin, J., Sadoul, B., Fiandrino, A., Covès, D., Callier, M. D., 2020. Integrated multi-trophic aquaculture of red drum (*Sciaenops ocellatus*) and sea cucumber (*Holothuria scabra*): Assessing bioremediation and life-cycle impacts. Aquaculture, 516. 734621 (17p.). doi.org/10.1016/j.aquaculture.2019.734621

Chen, J.-C., Lai, S.-H., 1993. Effects of temperature and salinity on oxygen consumption and ammonia excretion of juvenile *Penaeus japonicus* Bate. J. Exp. Mar. Bio. Ecol. 165, 161–170589. doi:10.1007/s10499-008-9169-7

Chopin, T., Cooper, J.A., Reid, G., Cross, S., Moore, C., 2012. Open-water integrated multi-trophic aquaculture: environmental biomitigation and economic diversification of fed aquaculture by extractive aquaculture. Rev. Aquac. 4, 209–220. doi:10.1111/j.1753-5131.2012.01074.x

Cook, E.J., Kelly, M.S., 2007. Enhanced production of the sea urchin *Paracentrotus lividus* in integrated open-water cultivation with Atlantic salmon *Salmo salar*. Aquaculture 273, 573–585. doi:10.1016/j.aquaculture.2007.10.038

Cubillo, A.M., Ferreira, J.G., Robinson, S.M.C.C., Pearce, C.M., Corner, R.A., Johansen, J., 2016. Role of deposit feeders in integrated multi-trophic aquaculture - A model analysis. Aquaculture 453, 54–66. doi:10.1016/j.aquaculture.2015.11.031

De Cubber, L., Lefebvre, S., Lancelot, T., Denis, L., & Gaudron, S. M., 2019. Annelid polychaetes experience metabolic acceleration as other Lophotrochozoans: Inferences on the life cycle of *Arenicola marina* with a Dynamic Energy Budget model. Ecological Modelling, 411. doi.org/10.1016/j.ecolmodel.2019.108773

495 Erler, D. V, Pollard, P.C., Burke, M., Knibb, W., 2000. Biological remediation of aqua-
496   culture waste: a combined finfish, artificial substrate treatment system, in:
497   Proceedings of the National Workshop of Wastewater Treatment and Integrated
498   Aquaculture. pp. 93–107.
499 Fang, J., Jiang, Z., Jansen, H.M., H U, F., Fang, J., Liu, Y., Gao, Y., Du, M., 2017.
500   Applicability of *Perinereis aibuhitensis* Grube for fish waste removal from fish
501   cages in Sanggou Bay, P. R. China. Ocean. Coast. Sea Res. 16, 294–304.
502   doi:10.1007/s11802-017-3256-1
503 Fidalgo e Costa, P., Narciso, L., Fonseca, L.C., 2000. Growth, survival and fatty acid
504   profile of *Nereis diversicolor* (O. F. Müller, 1776) fed on six different diets.
505   Bulletin of Marine Science, 67(1): 337–343.
506 Filgueira, R., Guyondet, T., Reid, G.K., Grant, J., Cranford, P.J., 2017. Vertical particle
507   fluxes dominate integrated multi-trophic aquaculture (IMTA) sites: implications
508   for shellfish − finfish synergy 9, 127–143.
509 Galasso, H.L., Callier, M. D., Bastianelli, D., Blancheton, J.-P., & Aliaume, C., 2017.
510   The potential of near infrared spectroscopy (NIRS) to measure the chemical
511   composition of aquaculture solid waste. Aquaculture, 476.
512   https://doi.org/10.1016/j.aquaculture.2017.02.035
513 Galasso, Helena Lopes, Richard, M., Lefebvre, S., Aliaume, C., & Callier, M. D., 2018.
514   Body size and temperature effects on standard metabolic rate for determining
515   metabolic scope for activity of the polychaete *Hediste (Nereis) diversicolor*.
516   PeerJ, 6. https://doi.org/10.7717/peerj.5675
517 Gillet, P., Mouloud, M., Durou, C., Deutsch, B., 2008. Response of *Nereis diversicolor*
518   population (Polychaeta, Nereididae) to the pollution impact – Authie and Seine
519   estuaries (France). Estuar. Coast. Shelf Sci. 76, 201–210.
520   doi:10.1016/j.ecss.2007.07.004
521 Hargrave, B.T. (Ed.), 2005. Environmental Effects of Marine Finfish Aquaculture,
522   Handbook of Environmental Chemistry. Springer-Verlag, Berlin/Heidelberg.
523   https://doi.org/10.1007/b12227
524 Hedman, J.E., Gunnarsson, J.S., Samuelsson, G., Gilbert, F., 2011. Particle reworking
525   and solute transport by the sediment-living polychaetes *Marenzelleria neglecta*
526   and *Hediste diversicolor*. J. Exp. Mar. Bio. Ecol. 407, 294–301.
527   doi:10.1016/j.jembe.2011.06.026
528 Heilskov, A.C.C., Holmer, M., 2001. Effects of benthic fauna on organic matter
529   mineralization in fish-farm sediments: importance of size and abundance. ICES
530   J. Mar. Sci. 58, 427–434. doi:10.1006/jmsc.2000.1026
531 Hopkins, K.D., 1992. Reporting Fish Growth: A Review of the Basics. Journal of the
532   World Aquaculture Society. 23, 173-179
533 Jansen, H. M., Broch, O. J., Bannister, R., Cranford, P., Handa, A., Husa, V., Jiang, Z.,
534   Strohmeier, T.,Strand, O., 2018. Spatio-temporal dynamics in the dissolved
535   nutrient waste plume from Norwegian salmon cage aquaculture. Aquaculture
536   Environment Interactions 10: 385-399.
537 Jiang, Z., Wang, G., Fang, J., Mao, Y., Bay, A., 2013. Growth and food sources of
538   Pacific oyster *Crassostrea gigas* integrated culture with Sea bass Lateolabrax.
539   Aquac. Int. 21, 45–52. doi:10.1007/s10499-012-9531-7
540 Kooijman, S. (2010). Dynamic Energy Budget theory for metabolic organisation.
541   Cambridge Univ. Press, Cambridge
542 Kooijman, S.A.L.M, Pecquerie L., Augustine S, Jusup, M., 2011. Scenarios for
543   acceleration in fish development and the role of metamorphosis. Journal of Sea
544   Research. 66, 4, 419–423

Katz, T., Herut, B., Genin, A., Angel, D.L., 2002. Gray mullets ameliorate organically enriched sediments below a fish farm in the oligotrophic Gulf of Aqaba (Red Sea). Mar. Ecol. Prog. Ser. 234, 205–214. doi:10.3354/meps234205

Kristensen, E., 1983. Ventilation and oxygen uptake by three species of *Nereis* (Annelida: Polychaeta). II. Effects of temperature and salinity changes. Mar. Ecol. Prog. Ser. 12, 299–306.

Lefebvre, S., Barille, L., Clerc, M., 2000. Pacific oyster (*Crassostrea gigas*) feeding responses to a fish-farm effluent. Aquaculture 187(1-2): 185-198.

Lefebvre, S., 2019. AmP *Hediste diversicolor*, version 2019/09/28

MacDonald, C.L.E., Stead, S.M., Slater, M.J., 2013. Consumption and remediation of European Seabass (*Dicentrarchus labrax*) waste by the sea cucumber *Holothuria forskali*. Aquac. Int. 21, 1279–1290. doi:10.1007/s10499-013-9629-6

Marques, B., Calado, R., Lillebø, A.I., 2017. New species for the biomitigation of a super-intensive marine fish farm effluent: Combined use of polychaete-assisted sand filters and halophyte aquaponics. Sci. Total Environ. 599–600, 1922–1928. doi:10.1016/j.scitotenv.2017.05.121

Mermillod-Blondin, F., Rosenberg, R., François-Carcaillet, F., Norling, K., Mauclaire, L., 2004. Influence of bioturbation by three benthic infaunal species on microbial communities and biogeochemical processes in marine sediment. Aquat. Microb. Ecol. 36, 271–284. doi:10.3354/ame036271

Meziane, T., Retiere, C., 2002. Growth of *Nereis diversicolor* (L.) juveniles fed with detritus of halophytes. Oceanol. Acta 25, 119–124.

Michaud, E., Desrosiers, G., Mermillod-Blondin, F., Bjorn Sundby, Georges Stora, 2006. The functional group approach to bioturbation: II. The effects of the *Macoma balthica* community on fluxes of nutrients and dissolved organic carbon across the sediment–water interface. Journal of Experimental Marine Biology and Ecology, 337, Issue 2, 178-189

Nelson, E.J., MacDonald, B. a. A., Robinson, S.M.C., 2012. The absorption efficiency of the suspension-feeding sea cucumber, *Cucumaria frondosa*, and its potential as an extractive integrated multi-trophic aquaculture (IMTA) species. Aquaculture 370–371, 19–25. doi:10.1016/j.aquaculture.2012.09.029

Nesto, N., Simonini, R., Prevedelli, D., Da, L., 2018. Evaluation of different procedures for fertilization and larvae production in *Hediste diversicolor* (O. F. Müller, 1776) doi:10.1111/are.13589

Nesto, N., Simonini, R., Prevedelli, D., Ros, L. Da, 2012. Effects of diet and density on growth, survival and gametogenesis of *Hediste diversicolor* (O. F. Müller, 1776) (Nereididae, Polychaeta). Aquaculture 362–363, 1–9. doi:10.1016/j.aquaculture.2012.07.025

Neori, A., Chopin, T., Troell, M., Buschmann, A.H., Kraemer, G.P., Halling, C., Shpigel, M., Yarish, C., 2004. Integrated aquaculture: rationale, evolution and state of the art emphasizing seaweed biofiltration in modern mariculture. Aquaculture 231, 361–391. doi:http://dx.doi.org/10.1016/j.aquaculture.2003.11.015

Nielsen, A.M., Eriksen, N.T., Iversen, J.J.L., Riisgård, H.U., 1995. Feeding, growth and respiration in the polychaetes *Nereis diversicolor* (facultative filter feeder) and *N. virens* (omnivorous) - a comparative study. Mar. Ecol. Prog. Ser. 125, 149–158. doi:10.3354/meps125149

Olive, P.J.W., Garwood, P.R.G., 1981. Gametogenic cycle and population structure of *Nereis (Hediste) diversicolor* and *Nereis (Nereis) pelagica* from north-east England. J. Maine Biol. Ass 61, 193–213.

595   Olivier, M., Desrosiers, G., Caron, A., Ret, 1996. Juvenile growth of the polychaete
596   *Nereis virens* feeding on a range of marine vascular and macroalgal plant
597   sources. Marine 125, 693–699.
598   Orr, L.C., Curtis, D.L., Cross, S.F., Gurney-Smith, H., Shanks, A., Pearce, C.M., 2014.
599   Ingestion rate, absorption efficiency, oxygen consumption, and fecal production
600   in green sea urchins (*Strongylocentrotus droebachiensis*) fed waste from
601   sablefish (*Anoplopoma fimbria*) culture. Aquaculture 422–423, 184–192.
602   doi:10.1016/j.aquaculture.2013.11.030
603   Ozoh, P.T.E., Jones, N. V, 1990. The effects of salinity and temperature on the toxicity
604   of copper to 1-day and 7-day-old larvae of *Hediste (Nereis) diversicolor* (O. F.
605   Müller). Ecotoxicol. Environ. Saf. 19, 24–32. doi:10.1016/0147-6513(90)90075-
606   G
607   Paltzat, D.L., Pearce, C.M., Barnes, P. a. A., McKinley, R.S., 2008. Growth and
608   production of California sea cucumbers (*Parastichopus californicus Stimpson*)
609   co-cultured with suspended Pacific oysters (*Crassostrea gigas* Thunberg).
610   Aquaculture 275, 124–137. doi:10.1016/j.aquaculture.2007.12.014
611   Papaspyrou, S., Thessalou-Legaki, M., Kristensen, E., 2010. The influence of infaunal
612   (*Nereis diversicolor*) abundance on degradation of organic matter in sandy
613   sediments.   J.   Exp.   Mar.   Bio.   Ecol.   393,   148–157.
614   doi:10.1016/j.jembe.2010.07.015
615   Porter, C.B., Krost, P., Gordin, H., Angel, D.L., 1996. Preliminary assessment of grey
616   mullet (*Mugil cephalus*) as a forager of organically enriched sediments below
617   marine fish farms. Isr. J. Aquac. Bamidgeh 48, 47–55.
618   Ren, J. S., Stenton-Dozey, J., Plew, D. R., Fang, J., & Gall, M., 2012. An ecosystem
619   model for optimising production in integrated multitrophic aquaculture systems.
620   Ecological Modelling, 246, 34–46. doi.org/10.1016/j.ecolmodel.2012.07.020
621   van Rijn, J. (2013). Waste treatment in recirculating aquaculture systems. Aquacultural
622   Engineering 53: 49-56.
623   Reid, G.K., Lefebvre, S., Filgueira, R., Robinson, S.M.C., Broch, O.J., Dumas A.,
624   Chopin, T.B.R., 2020. Performance measures and models for open-water
625   integrated multi-trophic aquaculture. Reviews in Aquaculture 12 (1), 47-75
626   Riisgård, H.U., 1994. Filter-feeding in the polychaete *Nereis diversicolor*: a review.
627   Netherlands J. Aquat. Ecol. 28, 453–458. doi:10.1007/BF02334216
628   Scaps, P., 2002. A review of the biology, ecology and potential use of the common
629   ragworm *Hediste diversicolor* (O. F. Müller) (Annelida: Polychaeta).
630   Hydrobiologia 470, 203–218. doi:10.1023/A:1015681605656
631   Trautmann, H., Mersmann, O., Arnu, D., 2011. cmaes: Covariance Matrix Adapting
632   Evolutionary Strategy. R package version 1.0-11. https://CRAN.R-
633   project.org/package=cmaes
634   Wang, H. Q., Seekamp, I., Malzahn, A., Hagemann, A., Carvajal, A. K., Slizyte, R.,
635   Standal, I. B., Handa, A., Reitan, K. I., 2019. Growth and nutritional
636   composition of the polychaete *Hediste diversicolor* (OF Muller, 1776) cultivated
637   on waste from land-based salmon smolt aquaculture. Aquaculture 502:232–241.
638   Wang, H. Q., Hagemann, A., Reitan, K. I., Handa, A., Uhre, M., Malzahn, A. M., 2020.
639   Embryonic and larval development in the semelparous Nereid polychaete
640   *Hediste diversicolor* (OF Muller, 1776) in Norway: Challenges and perspectives.
641   Aquaculture Research 00:1–17.
642   Watanabe, S., Kodama, M., Orozco, Z.G.A., Sumbing, J.G., Novilla, S.R.M., Lebata-
643   Ramos, M.J.H., 2015. Estimation of energy budget of sea cucumber, *Holothuria*
644   *scabra*, in integrated multi-trophic aquaculture., in: M. R. R. Romana-Eguia, F.

645   D. Parado-Estepa, N. D. Salayo, & M. J. H. Lebata-Ramos (Eds.), Resource
646   Enhancement and Sustainable Aquaculture Practices in Southeast Asia:
647   Challenges in Responsible Production of Aquatic Species: Proceedings of the
648   Internation. Tigbauan, Iloilo, Philippines Aquaculture Department, Southeast
649   Asian Fisheries Development Center, pp. 307–308
650 Wieser, W., 1973. Effects of Temperature on Ectothermic Organisms: Ecological
651   Implications and Mechanisms of Compensation, 1st ed. Springer-Verlag, New
652   York Heidelberg Berlin 1973.
653

654 Figure 1. DEB representation of allocation rule (κ rule) and energy fluxes in an
655 organism. Ingested energy is either assimilated or lost by defecation. Then part of the
656 energy mobilized from the reserve (κ) is allocated for somatic maintenance and growth,
657 and the remaining energy is spent for maturity and its associated maintenance. Once
658 sexual maturity is reached, the energy available for maturity is used for the production
659 of gametes (modified from Kooijman, 2010).
660
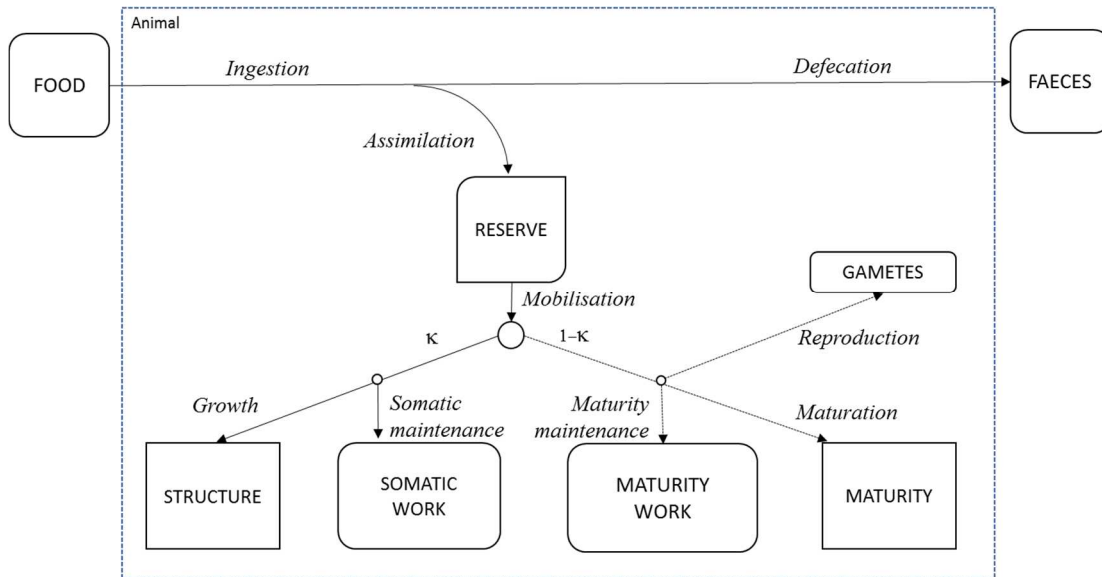
661
662
663
664

665   Figure 2. *Hediste diversicolor*. Comparison of DEB simulation (line) and growth data
666   (a) L3 length (cm) and (b) wet weight (WW) (g) for polychaetes fed with Fish faeces
667   and Fish feed. After optimization, f=0.5 for Fish feed and f=0.6 for Fish faeces. Before
668   the experiment (dashed line), f was estimated to be 0.4. Individual WW was measured
669   on days 177 and 211, and individual L3 length on days 113, 144, 177 and 211. The
670   values obtained during the last biometry (211 days post-fertilization) were not included
671   in the optimization due to high suicide reproduction. MRE = 0.11 for L3 length values.
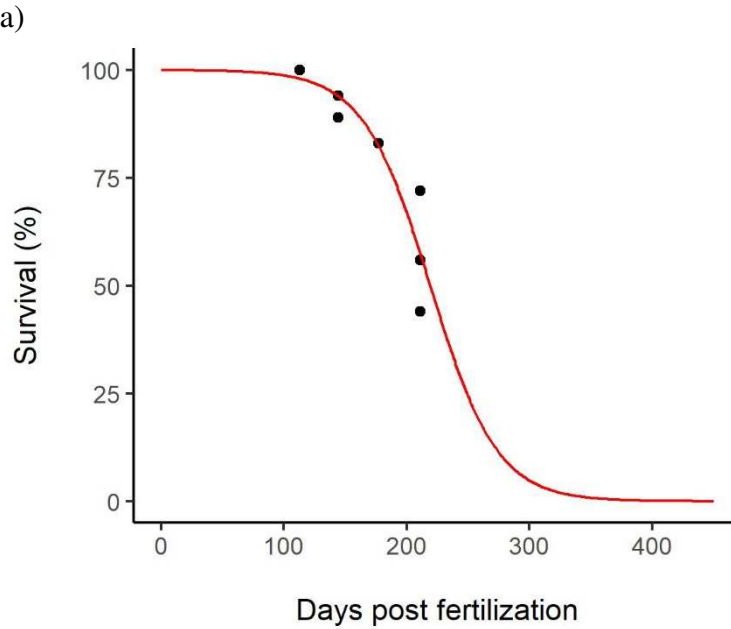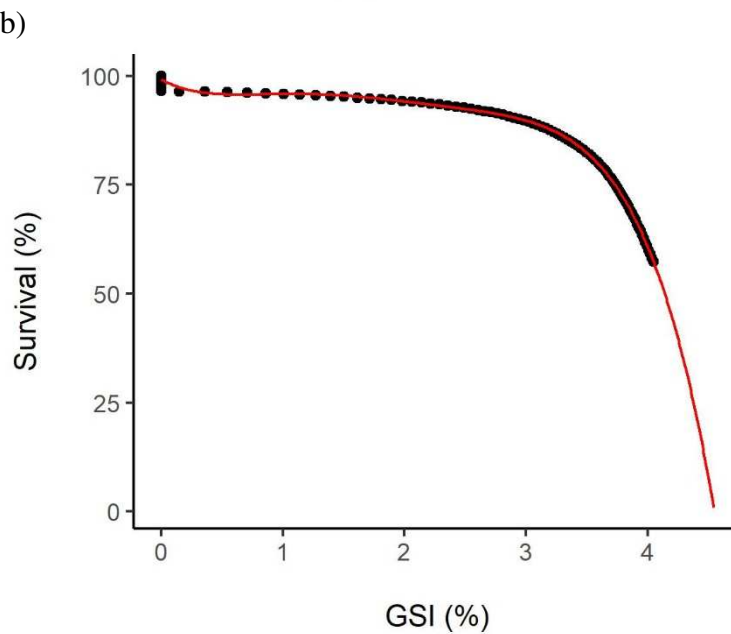
672   a)

673
674   b)
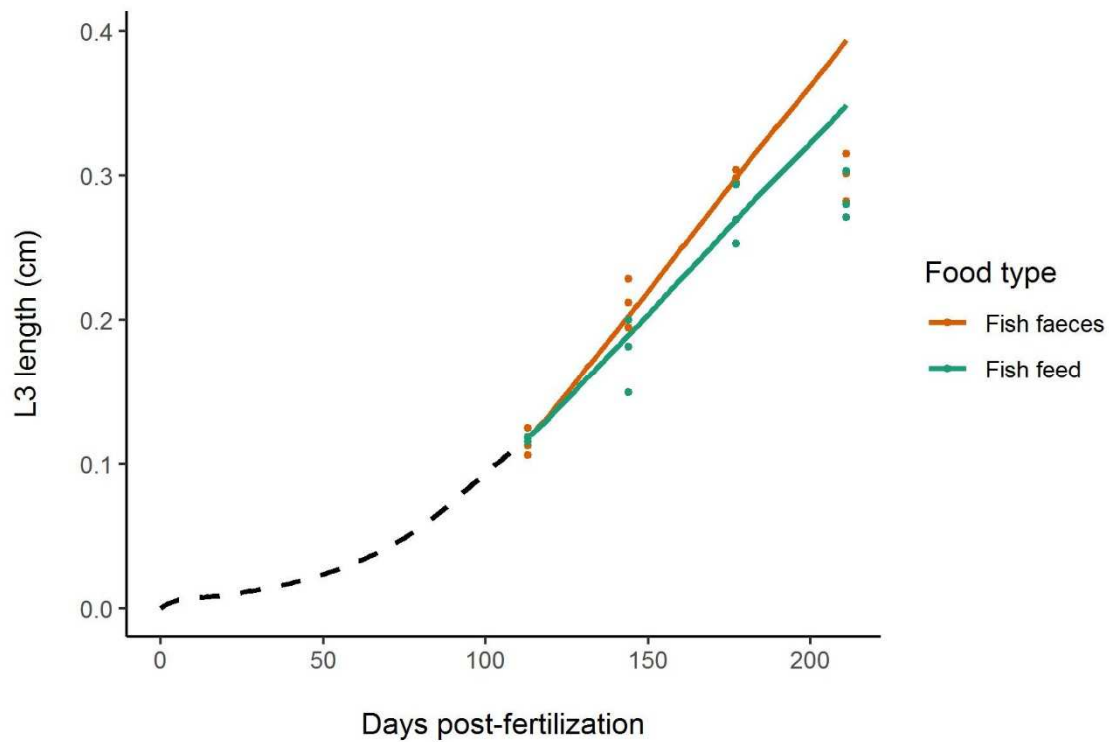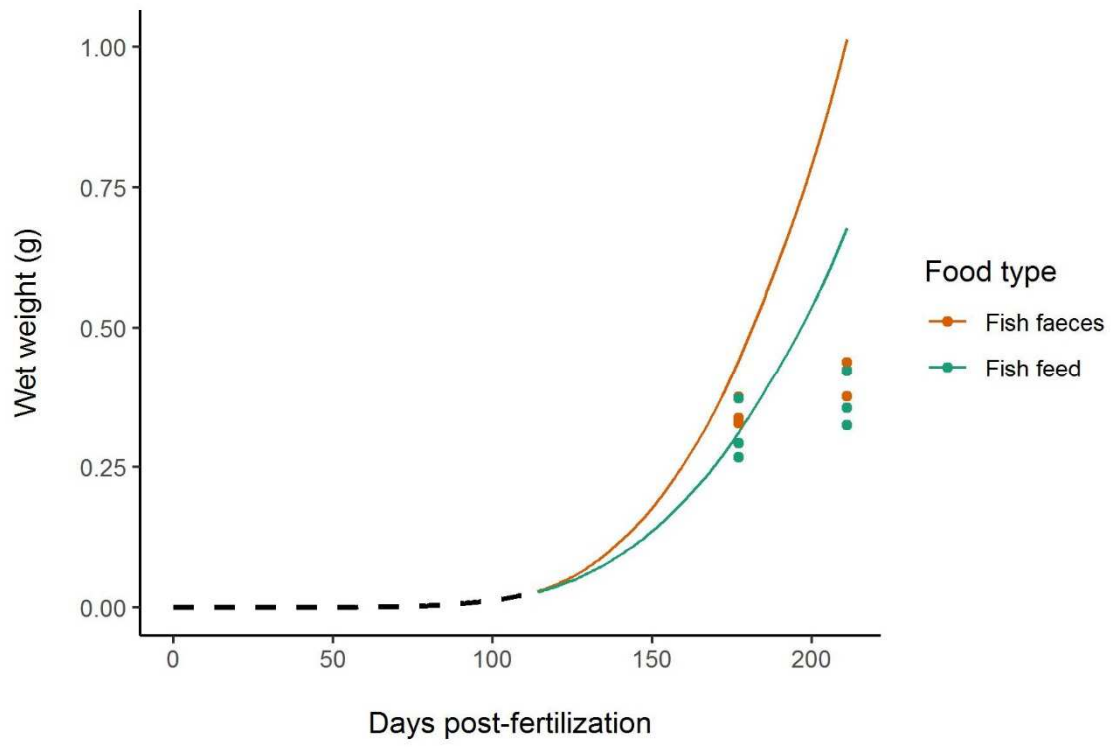
677 Figure 3. Survival over time and by GSI in polychaetes fed with fish faeces. (a) Survival
678 over time. The curve was fitted using a sigmoid (red line, $R^2 = 0.87$). (b) Survival by
679 estimated GSI from the DEB model on ages ranging from 0 to 500 days post-
680 fertilization. A polynomial function of degree 5 was fitted (red line, $R^2 = 1$).
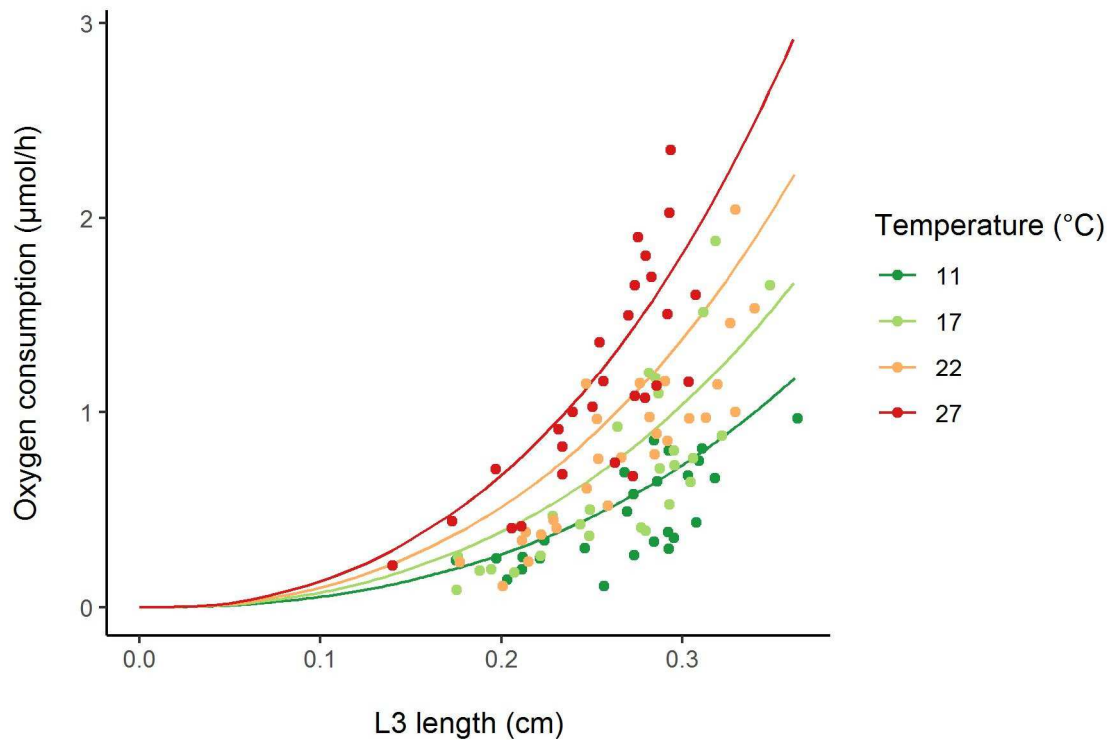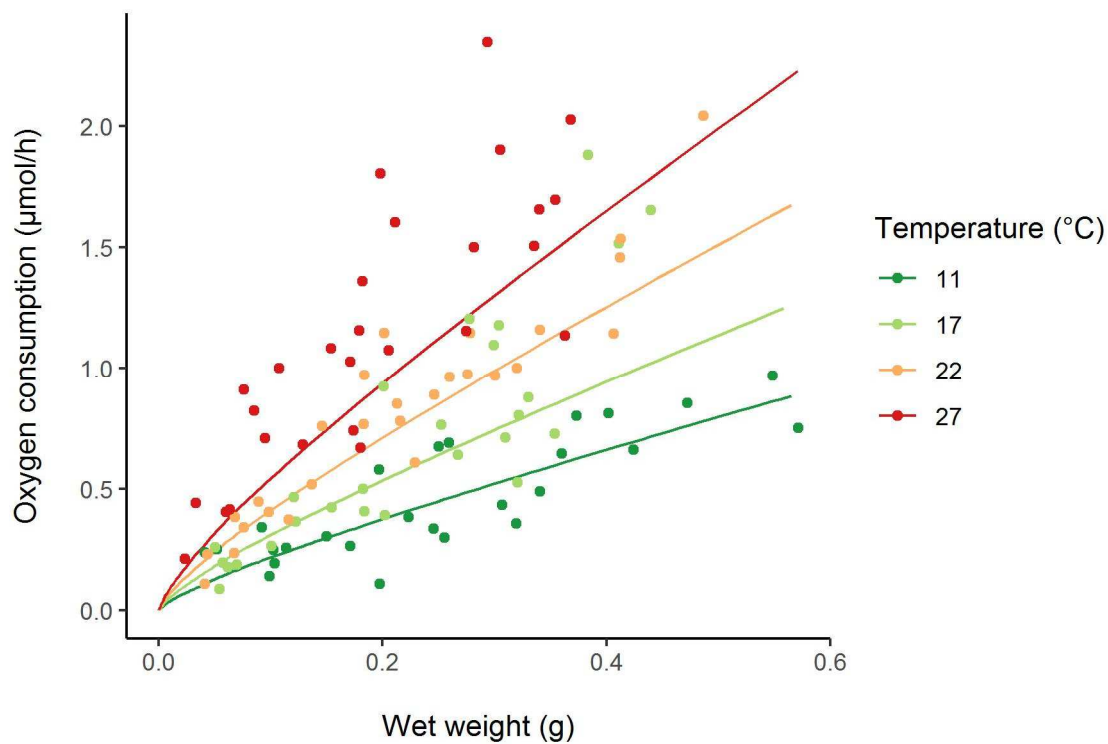681
682 a)

683
684 b)

685
686
687
688

689   Figure 4. *Hediste diversicolor*. Comparison of DEB simulation (line) and oxygen
690   consumption rates at four temperatures (11°C, 17°C, 22°C and 27°C) expressed over (a)
691   L3 length (cm) and (b) wet weight (WW) (g) for polychaetes fed with fish faeces (*f*
692   =0.6). MRE = 0.51 for L3 length and WW values.

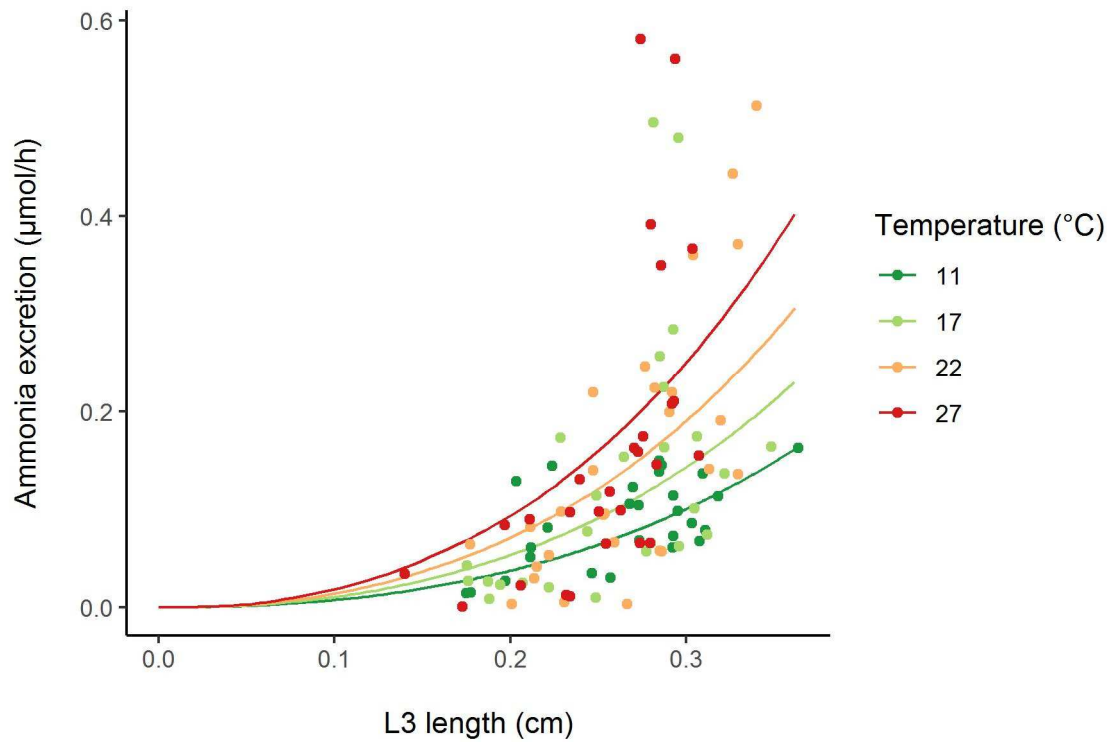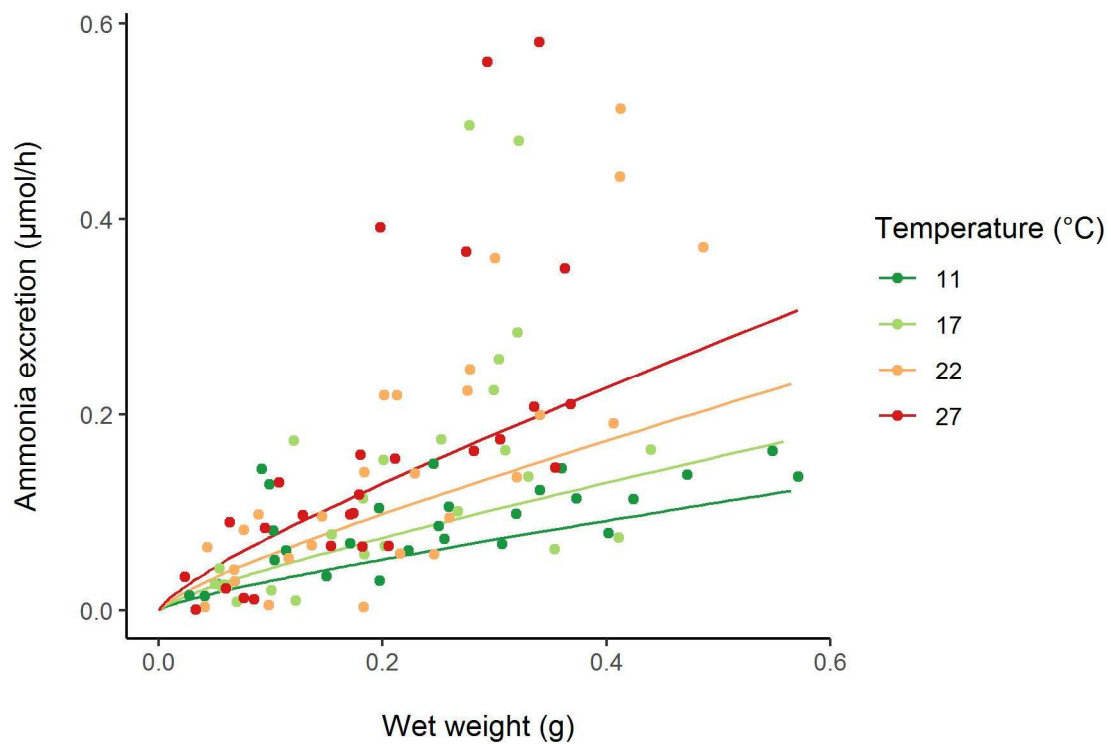693   a)

694
695   b)

696
697

698 Figure 5. *Hediste diversicolor*. Comparison of DEB simulation (line) and ammonia
699 excretion rates at four temperatures (11°C, 17°C, 22°C and 27°C) expressed over (a) L3
700 length (cm) and (b) wet weight (WW) (g) for polychaetes fed with fish faeces (*f* =0.6).
701 MRE = 0.8 for L3 length and WW values.

702 a)

703
704 b)

705
706

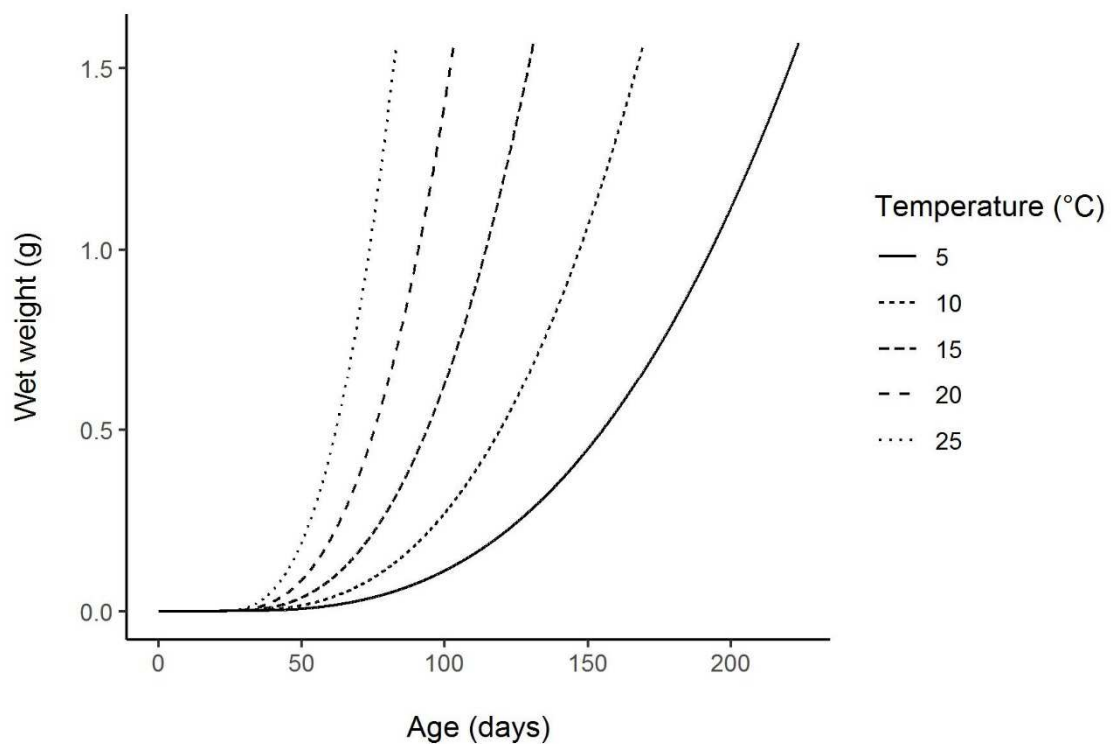707 Figure 6. DEB simulations of *H. diversicolor* individual growth in L3 length (cm) and
708 wet weight (WW) (g) with temperatures ranging from 5°C to 25°C. Simulations were
709 performed until the maximum observed size (1.57 g, Add my Pet database, Lefebvre,
710 2019) (based on the literature) was reached. The functional scaled response was
711 maintained constant at *f*=1.

712 a)

713
714 b)
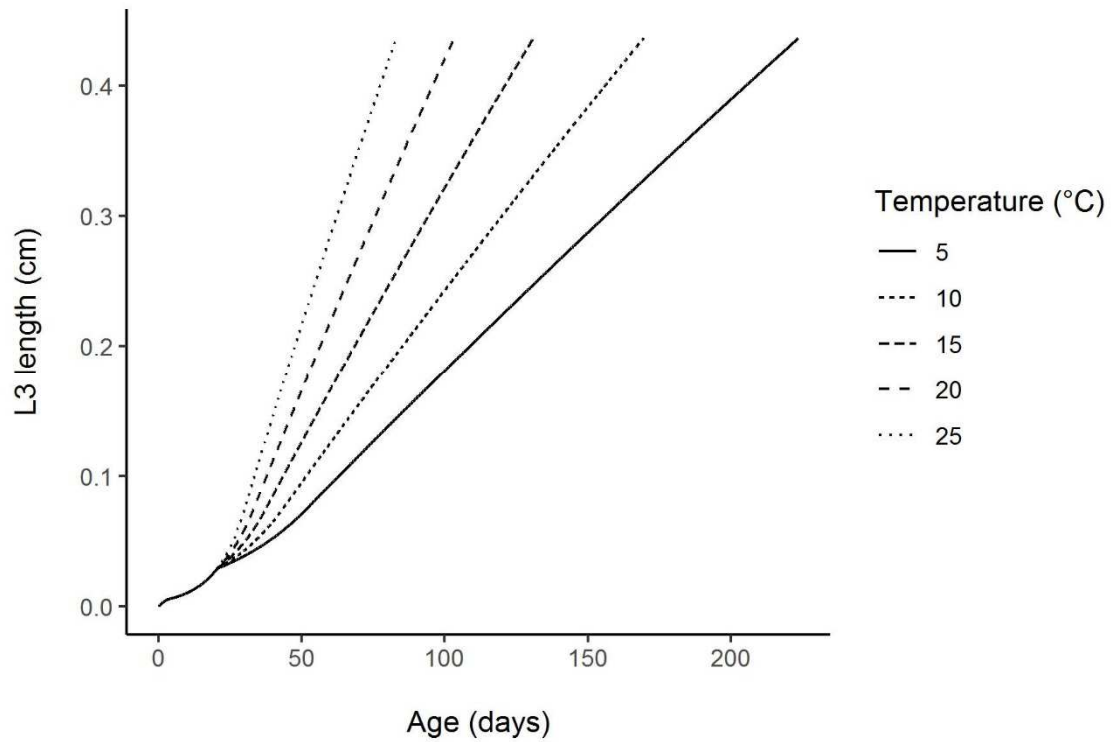
715

716 Figure 7. DEB simulations of *H. diversicolor* individual growth in a) L3 length (cm)
717 and b) wet weight (WW) (g) over time (days) according to different food abundance
718 (scaled functional response, *f*) scenarios. Simulations were performed until the GSI for
719 first reproduction was reached (3%). The temperature was maintained constant at 20°C.
720 *f* at 0.5 means that individuals were fed at 50% of *ad libitum*.

721 a)
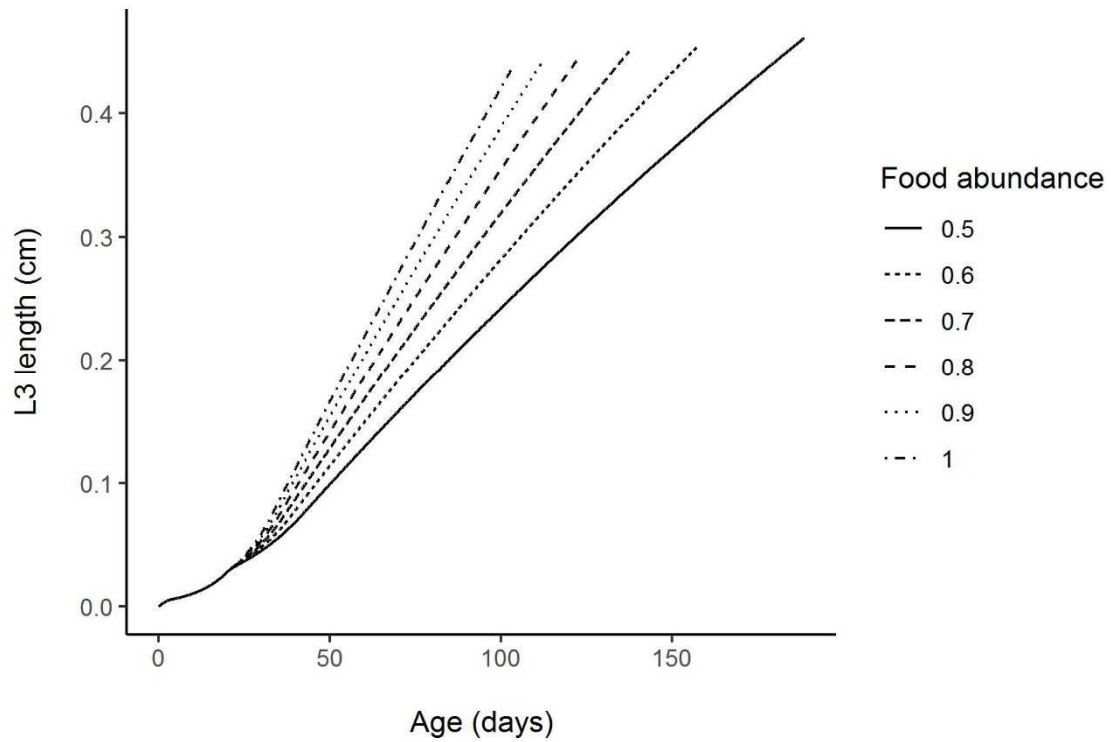
722
723 b)

724
725
726

727   Table 1. DEB abj-model parameters estimated for the polychaete *Hediste diversicolor*
728 (Lefebvre, 2019, Add-my-Pet database).

729

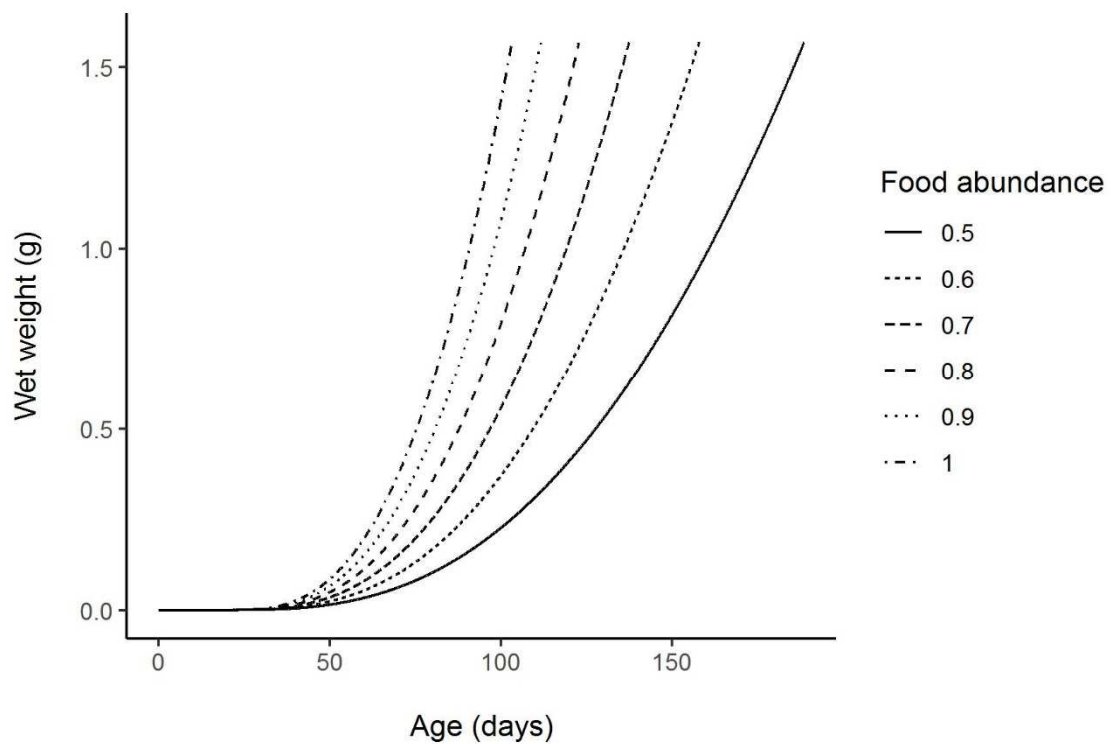| Parameters	Value	Unit	Description
L_m	0.53073	Cm	Maximum volumetric length
$\{\dot{p}_{Am}\}$	14.3197	J cm^{-2} d^{-1}	Maximum surface-specific assimilation rate
$\dot{v}$	0.01123	cm d^{-1}	Energy conductance (velocity)
g	2.761754	-	Energy investment ratio
$\dot{k}_J$	0.002	d^{-1}	Maturity maintenance rate coefficient
$\dot{k}_M$	0.007663691	d^{-1}	Somatic maintenance rate
κ	0.96018	-	Allocation fraction to soma
κ_R	0.95	-	Reproduction efficiency
$[\dot{p}_M]$	25.91	J cm^{-3} d^{-1}	Volume specific somatic maintenance rate
$[E_G]$	3380.46	J cm^{-3}	Volume specific costs of structure
E_H^b	0.0003164	J	Energy maturity at birth
E_H^j	0.7665	J	Energy maturity at metamorphosis
E_H^p	7.883	J	Energy maturity at puberty
T_A	4877.15	K	Arrhenius temperature
T_{ref}	293.15	K	Reference temperature
ω	0.440695	-	Contribution of reserve to body weight or physical volume
δ_M	2.3579	-	Shape coefficient for L3 length
η_{OA}	0.329	µmol-O$_2$ J^{-1} d^{-1}	Energy-oxygen coupling coefficient for the assimilation flux
η_{OD}	1.977	µmol-O$_2$ J^{-1} d^{-1}	Energy-oxygen coupling coefficient for the dissipation flux
η_{OG}	0.285	µmol-O$_2$ J^{-1} d^{-1}	Energy-oxygen coupling coefficient for the growth flux
η_{NA}	0.045	µmol-NH$_3$ J^{-1} d^{-1}	Energy-ammonia coupling coefficient for the assimilation flux
η_{ND}	0.273	µmol-NH$_3$ J^{-1} d^{-1}	Energy-ammonia coupling coefficient for the dissipation flux
η_{NG}	0.039	µmol-NH$_3$ J^{-1} d^{-1}	Energy-ammonia coupling coefficient for the growth flux

730
731
732

733 Table 2. Growth performance of *Hediste diversicolor* fed with fish faeces and
734 commercial fish feed over time (age in days), and associated means of L3 length (cm),
735 wet weight (WW g) and survival: n = number of observations and SD = standard
736 deviation. Statistical analysis was performed with food type as fixed factor and tank as
737 random factor (* when $p < 0.05$).
738

Age (days)	Food type	n	L3 ± SD (cm)	WW ± SD (g)	Survival (%)
113	Fish faeces	54	0.11 ± 0.02		
	Fish feed	54	0.12 ± 0.02		
144	Fish faeces	50	0.21 ± 0.05		93
	Fish feed	52	0.18 ± 0.05		96
177	Fish faeces	45	0.30 ± 0.05*	0.35 ± 0.16	83
	Fish feed	42	0.27 ± 0.05*	0.30 ± 0.18	78
211	Fish faeces	31	0.30 ± 0.05	0.41 ± 0.17	57
	Fish feed	26	0.28 ± 0.06	0.36 ± 0.15	48

739
740
741

742 Table 3. Effects of temperature and scaled functional response (f=0.5, f=0.6 and f=1 at
743 20°C; 5°C and 25°C with f=1) on *H. diversicolor* L3 length (cm), wet weight (WW g)
744 and total assimilated energy (Assim in J) and faeces assimilation (g DW). Total
745 assimilated energy was estimated over ragworm production cycle (see Wang et al. 2020
746 for production cycle description). A production cycle was stopped when GSI reached
747 3%, or when WW reached 0.5 g WW (minimum polychaete market weight). The
748 bioremediation capacity of one individual was estimated by transforming the
749 assimilated energy in fish faeces by assuming (based on the literature) that 1 g of fish
750 faeces represents 10.4 kJ. A population density of 3700 ind.m^{-2} (Scaps, 2002) was
751 chosen to estimate the bioremediation capacity of a ragworm farm per m^2 and year.

752
753

T	f	age	L3	WW	GSI	Surv	Assim (per ind.)			Bioremediation	
(°C)		days	cm	g	%	%	J cycle^{-1}	J yr^{-1}	g (DW) yr^{-1}	g (DW) m^{-2} yr^{-1}	kg (DW) 100m^{-2} yr^{-1}
up to 3% GSI											
20	0.5	99	0.24	0.2	3.0	90	641	2370	0.23	755	75
20	1	79	0.31	0.6	3.0	90	1603	7443	0.72	2370	237
5	1	163	0.31	0.6	3.0	90	1596	3572	0.34	1137	114
25	1	64	0.31	0.6	3.0	90	1600	9067	0.87	2887	289
up to 0.5 g WW											
20	0.5	128	0.32	0.5	3.9	67	1536	4390	0.42	1039	104
20	1	75	0.30	0.5	2.9	90	1363	6598	0.63	2122	212
5	1	155	0.30	0.5	2.9	90	1355	3187	0.31	1025	103
25	1	62	0.30	0.5	2.9	90	1362	8020	0.77	2579	258

754